Acoel Single-Cell Transcriptomics: Cell Type Analysis of a Deep Branching Bilaterian

Jules Duruz,[1] Cyrielle Kaltenrieder,[1] Peter Ladurner,[2] Rémy Bruggmann,[3,4] Pedro Martìnez,*[,5,6] and Simon G. Sprecher*[,1]

[1]Department of Biology, Institute of Zoology, University of Fribourg, Fribourg, Switzerland
[2]Institute of Zoology and Center of Molecular Bioscience Innsbruck, University of Innsbruck, Innsbruck, Austria
[3]Institute of Cell Biology, University of Bern, Bern, Switzerland
[4]Interfaculty Bioinformatics Unit, University of Bern, Bern, Switzerland
[5]Departament de Genètica, Universitat de Barcelona, Barcelona, Catalonia, Spain
[6]Institut Català de Recerca i Estudis Avancats (ICREA), Passeig de Lluís Companys, Barcelona, Spain

***Corresponding authors:** E-mails: pedro.martinez@ub.edu; simon.sprecher@unifr.ch.

Associate editor: Mary O'Connell

Abstract

Bilaterian animals display a wide variety of cell types, organized into defined anatomical structures and organ systems, which are mostly absent in prebilaterian animals. Xenacoelomorpha are an early-branching bilaterian phylum displaying an apparently relatively simple anatomical organization that have greatly diverged from other bilaterian clades. In this study, we use whole-body single-cell transcriptomics on the acoel *Isodiametra pulchra* to identify and characterize different cell types. Our analysis identifies the existence of ten major cell type categories in acoels all contributing to main biological functions of the organism: metabolism, locomotion and movements, behavior, defense, and development. Interestingly, although most cell clusters express core fate markers shared with other animal clades, we also describe a surprisingly large number of clade-specific marker genes, suggesting the emergence of clade-specific common molecular machineries functioning in distinct cell types. Together, these results provide novel insight into the evolution of bilaterian cell types and open the door to a better understanding of the origins of the bilaterian body plan and their constitutive cell types.

Key words: **bilaterians, Xenacoelomorpha, single-cell transcriptomics.**

Article

Introduction

The emergence and early diversification of bilaterians remains a widely debated subject. Identification and characterization of cell types that make up animals are key to understanding the diversity of bilaterian tissues and morphologies. The recent advent of single-cell transcriptomics provides a unique technical entry point to view the expression profile of individual cells, enabling us to investigate cell type identities in various organisms.

Xenacoelomorpha are a recently established phylum of bilaterians (Philippe et al. 2011) whose phylogenetic position has long been a source of debate, because of extreme morphological diversity within the phylum, particularities in their anatomy, and the fast-evolutionary rate of their genomes. Some anatomical features of the Xenacoelomorpha appear similar to nonbilaterian clades such as the absence of a through-gut, the lack of a coelom, the sole use of cilia for locomotion, and the apparent lack of an excretory system. However, the Xenacoelomorpha display some core bilaterian features such as a centralized nervous system with diverse levels of organization. Mature Xenoturbellida appear to lack a clearly identifiable central nervous system (Raikova et al. 2000), whereas many members of the subgroup Acoelomorpha contain centralized brains and various amounts of nerve cords (Achatz and Martinez 2012; Martínez et al. 2017). The variability of tissue architectures has also been demonstrated for other tissues such as the musculature, the mouth and pharynxes, and the copulatory organs (Jondelius et al. 2011; Perea-Atienza et al. 2013). This apparent flexibility of tissue organization is prominent within the Xenacoelomorpha and highlights the uniqueness of the clade for understanding the mechanisms that regulate the evolution of morphologies and their constitutive building units: the cell types.

Because their anatomical and morphological features seem to share characteristics with those of both cnidarians and bilaterians, this phylum has been at the center of an ongoing debate regarding their use as proxies for an ancestral bilaterian (Baguñà and Riutort 2004; Baguñà et al. 2008; Cannon et al. 2016). Acoelomorphs had been initially thought to be plathelminths due to their similar superficial aspect, but later genetic analysis placed them either as sister group to the remaining bilaterians (Ruiz-Trillo et al. 1999) or within

deuterostomes, as a sister group to Ambulacraria (Philippe et al. 2011). A later study taking into account supplementary genomic and transcriptomic data from several species and refined evolutionary models placed Xenacoelomorpha as a sister group to all other Bilaterians (Nephrozoa) making it a candidate phylum to better understand bilaterian origins (Cannon et al. 2016). The use of alternative models of gene evolution has questioned that phylogenetic position (Philippe et al. 2019). In fact, these alternative suggestions of phylogenetic affinities reflect general methodological problems involved in the use of phylogenomic tools and models to reconstruct early diverging clades (Kapli et al. 2020), a problematic that remains unsolved with current approaches.

Few species of acoels (Acoela) have so far been kept in laboratory conditions and used for research. The acoels *Symsagittifera roscoffensis*, *Hofstenia miamia*, and *Convolutriloba longifissura* have been used to study photosymbiosis (Dupont et al. 2012; Nissen et al. 2015; Arboleda et al. 2018), regeneration (Perea-Atienza et al. 2013; Bailly et al. 2014; Srivastava et al. 2014; Sprecher et al. 2015; Gehrke et al. 2019), nervous system morphology and development (Bery et al. 2010; Semmler et al. 2010; Perea-Atienza et al. 2018; Hulett et al. 2020), and body patterning (Hejnol and Martindale 2008a, 2008b, 2009; Martindale and Hejnol 2009; Moreno et al. 2009). A particularly interesting, and tractable, system is the acoel *Isodiametra pulchra*. Since its original description (Smith and Bush 1991), the use of this species in the laboratory has been gaining acceptance because of their easy maintenance and of the availability of different technologies, from in situ and immunochemistry to the gene knockdown using RNAi interference (De Mulder et al. 2009; Moreno et al. 2010), mitochondrial genome sequence (Robertson et al. 2017), and transcriptome sequences (Cannon et al. 2016; Brauchle et al. 2018). *Isodiametra pulchra* has been instrumental in developing many key studies of the Xenacoelomorpha particularly in the description of cell types by characterizing the expression patterns of specific genes. Detailed descriptions of stem-like cells were done by showing the expression of the stem cell marker *piwi-like 1* and *piwi-like 2* in the neoblasts and germ cells of *I. pulchra* (De Mulder et al. 2009). The nervous system of *I. pulchra* was thoroughly described at a morphological level using immunohistochemistry as well as electron microscopy (Achatz and Martinez 2012). Additionally, the expression of key genes involved in dorsoventral nerve cord patterning was also shown by in situ hybridization (ISH) (Martín-Durán et al. 2018). Many different neuropeptides were also identified in *I. pulchra* and predict important neuronal diversity in these organisms (Thiel et al. 2018). Different studies of the mesoderm in *I. pulchra* described the expression patterns of known mesodermal genes (Ladurner and Rieger 2000; Rieger and Ladurner 2003; Chiodin et al. 2013). More specifically, some cell type markers could be identified such as *tropomyosin* and *LIMmuscle* that were confirmed to be specific to muscle cells, the transcription factors *foxA2* and *foxC* that were shown to have subepidermal expression and the *twist 1* and *twist 2* genes were shown to be expressed in neoblasts (Chiodin et al. 2013). In addition, proposed excretory-like cells were shown to express ammonia transporter such as *rhesus*, *nka*, and *v-ATPase B* as well as different types of aquaporins in digestive-associated cells, subepidermal cells, and neural cells (Andrikou et al. 2019).

Recent advances in single-cell RNA sequencing technologies have enabled the thorough description of the full repertoire of cell types (cell atlas) of various organisms by defining cell types as groups of cells clustered based on their RNA expression profiles. This has been done in many animals including both nonbilaterians (Sebe-Pedros, Chomsky, et al. 2018; Sebe-Pedros, Saudemont, et al. 2018; Siebert et al. 2019) as well as some bilaterian "model" organisms, for instance: the planarian *Schmidtea mediterranea* (Fincher et al. 2018; Plass et al. 2018; Swapna et al. 2018), *Drosophila melanogaster* (Karaiskos et al. 2017), *Mus musculus* (Han et al. 2018), the nematode *Caenorhabditis elegans* (Packer et al. 2019), and the annelid *Platynereis dumerilii* (Achim et al. 2018) among others. These different studies have all revealed a surprising level of cell type heterogeneity and the presence of previously unknown cell types in these animals.

In this study, we deep-sequenced whole *I. pulchra* hatchlings at a single-cell resolution to reveal the diversity of cell types in this representative of the enigmatic phylum Xenacoelomorpha with the aim of understanding how these different cells contribute to the organization of its specific body plan. We find a rich diversity of cell types corresponding to well-known bilaterian tissues. Particularly remarkable is the diversity within the nervous system of *I. pulchra*. We further describe cells involved in diverse metabolic activities such as digestion and excretion that could complement the described function of the digestive syncytium: a large polynucleated cell that had to be excluded from our single-cell sequencing because of its large size and shape. Interestingly, we find a variety of putative secretory cells that may play a role in defense and innate immunity and others that are putatively involved in the secretion of adhesive substances. Interestingly, although most cell types of *I. pulchra* express well-known cell type markers shared with other animal clades we also observe large numbers of coexpressed genes, which appear only to be present in Xenacoelomorpha (*S. roscoffensis* and *Xenoturbella bocki*) suggesting the presence of a phylum-specific group of genes contributing to the establishment of cell type identities among the Xenacoelomorpha.

Results

Transcriptome Analysis of *Isodiametra pulchra* Highlights Divergence from Other Animal Clades

In order to enable efficient cell type analysis of *I. pulchra*, we reanalyzed and annotated its previously published transcriptome (Brauchle et al. 2018) using trinotate (Bryant et al. 2017). To allow for better mapping of the reads obtained in single-cell RNA sequencing experiments, redundancy of the transcriptome was reduced by clustering highly similar sequences that are considered to be transcription isoforms using Corset (Davidson and Oshlack 2014). The final number of transcripts could therefore be reduced from 320,563 to 45,515 genes in our so-called nonredundant transcriptome.

Completeness of the transcriptome was tested by searching for the 978 BUSCOs (Benchmarking Universal Single Copy Orthologs, Simão et al. 2015; Seppey et al. 2019; v3.0.2) defined for the Metazoa in the transcriptome. Out of these 978 genes, 732 were found in our nonredundant transcriptome, either as a single-copy or as duplicated genes, 61 were fragmented, and 185 were not found (supplementary fig. S1B, Supplementary Material online). This corresponds to an estimation of 74.8% of BUSCO groups that could be identified in our nonredundant transcriptome, either as a single-copy or as duplicated genes. The list of missing BUSCOs is available in supplementary table 3, Supplementary Material online. As a comparison, we performed the same analysis on the original transcriptome (Brauchle et al. 2018) and obtained better results with 326 single-copy, 542 duplicated BUSCOs, 25 fragmented, and 85 missing. This showed a higher proportion of identified BUSCOs (88.7%) but with a very high proportion of duplicated genes (55.4%), confirming the important redundancy of this transcriptome.

Functional annotation of the nonredundant transcriptome was performed by comparing *I. pulchra* sequences with a protein database (Swissprot) using BlastX (version 2.7.1) and conserved protein domains were identified by comparing *I. pulchra* predicted protein sequences with a database of curated protein domains (Pfam). Less than half of the *I. pulchra* transcripts had clear similarities to proteins of the database (e-value ≤ 0.01) and/or a predicted protein domain. The annotation reveals that the *I. pulchra* transcriptome contains 20,446 sequences with orthologous in other organisms leaving 25,069 transcripts of unknown identity (supplementary fig. S1C, Supplementary Material online). About 17,810 transcripts encode for a protein (Open reading frame) with a conserved structural domain. The others might correspond to acoel-specific or highly divergent sequences. To assess the conservation of these unknown genes/sequences within the Xenacoelomorpha and verify that they are not a contamination of our transcriptome, we compared these sequenced with the transcriptomes generated for *S. roscoffensis* and *X. bocki* (Brauchle et al. 2018) using BLAST (version 2.7.1). This process identified 4,332 transcripts that have orthologs in *S. roscoffensis* (e-value ≤ 0.01) and therefore may be acoel-specific and 3,063 transcripts that have orthologs in *X. bocki* (e-value ≤ 0.01) and might therefore be Xenacoelomorpha-specific (supplementary fig. S1A, Supplementary Material online). A list of those genes is provided in supplementary tables 4 and 5, Supplementary Material online.

Isodiametra pulchra Single-Cell Transcriptomes Depict a Repertoire of Ten Major Cell Type Categories

Two separate single-cell RNA sequencing (scRNAseq) experiments were conducted and later batched together in order to ensure a larger number of cells and the presence of one biological replicate. The analysis of scRNAseq data of whole *I. pulchra* hatchlings resulted in an estimate of 14,864 recovered cells, after aggregation of the two experiments, corresponding approximately to a 14× coverage of the expected cell number in a whole hatchling that we estimated to be in the range of 900–1,000 cells. This latter approximation was determined by performing automated counting of nuclei stained with DAPI in confocal microscopy stack of a whole hatchling (fig. 1C). The median unique molecular identifiers and gene-per-cell estimates were of 608 and 405, respectively, with a total of 21,597 genes detected. The unique molecular identifier values are consistent with those of other studies, with the understanding that these numbers are extremely variable from one species to the other and sometimes even from one experimental condition to another in the same species (Fincher et al. 2018; Sebe-Pedros, Chomsky, et al. 2018; Sebe-Pedros, Saudemont, et al. 2018; Swapna et al. 2018). The mean reads per cell was of 49,404 postnormalization. The data were filtered to only include cells with a gene-per-cell count over 200 to exclude cells of poor quality and under 2,000 to exclude possible sequencing of several cells aggregated together (supplementary fig. S2A and B, Supplementary Material online). Cells were clustered using 25 principal components selected in base of the assessment of an elbow plot that ranks principal components according to the percentage of variance that they explain (Satija et al. 2015; supplementary fig. S2C, Supplementary Material online) and with a resolution of 2.5. This resulted in the detection of a total of 42 clusters. Identity was assigned to these clusters by analyzing the best markers of each cluster, which are the genes that were most differentially upregulated in one specific cluster with respect to all others.

Clusters were manually annotated and fitted into ten categories defined based on the predicted function of identified markers (fig. 1A) which also included a category of uncharacterized cell types. In addition, we identified what appeared to be prokaryotic sources, based on the identification of some bacterial rRNA sequences. These prokaryotic sequences could reflect the presence of endosymbionts in *I. pulchra*, since the same transcripts were found in both the single-cell pools and the RNA sequences used for transcriptome assembly. However, the presence of various possible contaminants in these clusters mixed with *I. pulchra* sequences raises the possibility that these cells are recurrent contamination of the medium or are part of organisms that were ingested by the animal. For these reasons, we excluded these cells for the cell type analysis, therefore keeping only the cell types that are confidently of animal origin. The remaining 41 clusters used in this study are shown on supplementary figure S2, Supplementary Material online and the genes differentially expressed in each cluster are provided in the supplementary table 2, Supplementary Material online. A few representative markers of each category were plotted to visually assess their enrichment within each cell cluster (fig. 1B). Defined categories include stem-cells, neurons, two distinct types of digestive cells, two distinct types of epithelial cells, secretory cells, and muscle cells.

Stem Cells Express Piwi-Like Genes and Conserved Proliferation Markers

An interesting problematic in the field of stem cell biology is the putative convergence of neoblast phenotypes in the Platyhelminthes and the Acoela. Here, we address this topic by analyzing the expression of two previously characterized

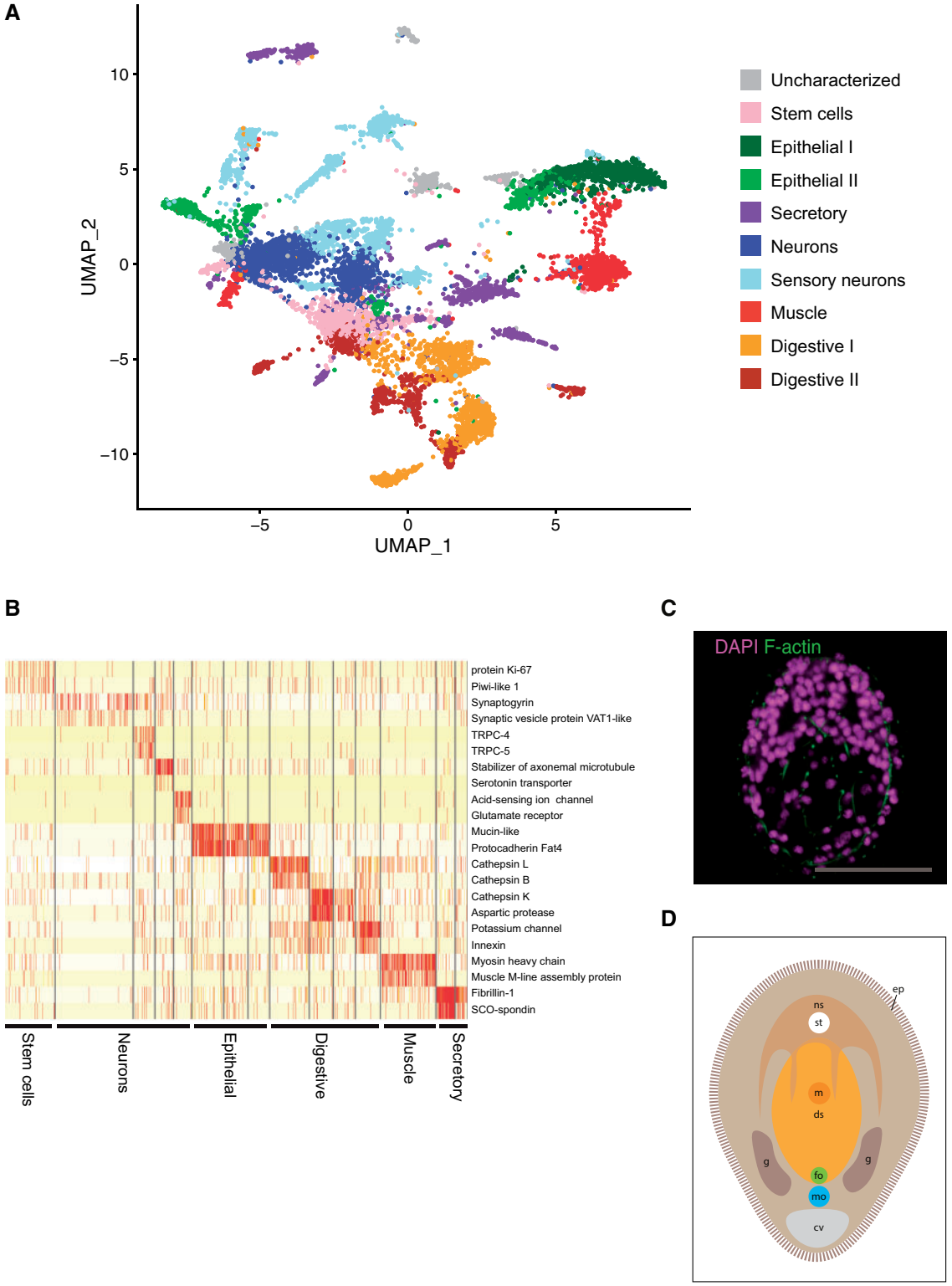

Fig. 1. Clustering of *Isodiametra pulchra* cells depicts a repertoire of ten major cell type categories. (*A*) UMAP of all cells showing the assignment of all 41 cell clusters to cell type categories. (*B*) Heatmap showing the expression of cell type-specific markers for some of the cell categories. (*C*) Confocal image showing DAPI staining of nuclei in an *I. pulchra* hatchling (magenta) and phalloidin staining of actin fibers (green). Anterior side is up. Scale bar = 50 μM. (*D*) Scheme of the *I. pulchra* hatchling showing the epidermis (ep), nervous system (ns), statocyst (st), mouth opening (m), digestive syncytium (ds), developing gonads (g), female reproductive organ (fo), male reproductive organ (mo), and choroid vacuole (cv).

stem cell markers for *I. pulchra piwi-like 1* and *piwi-like 2* (De Mulder et al. 2009) that were shown to be expressed in the stem cells of *I. pulchra* as well as in the germ cells of both adults and juveniles. The analysis of cell clusters uncovered a population of cells with stem cell-like profiles based on the broad expression of the two markers *piwi-like 1* and *piwi-like*

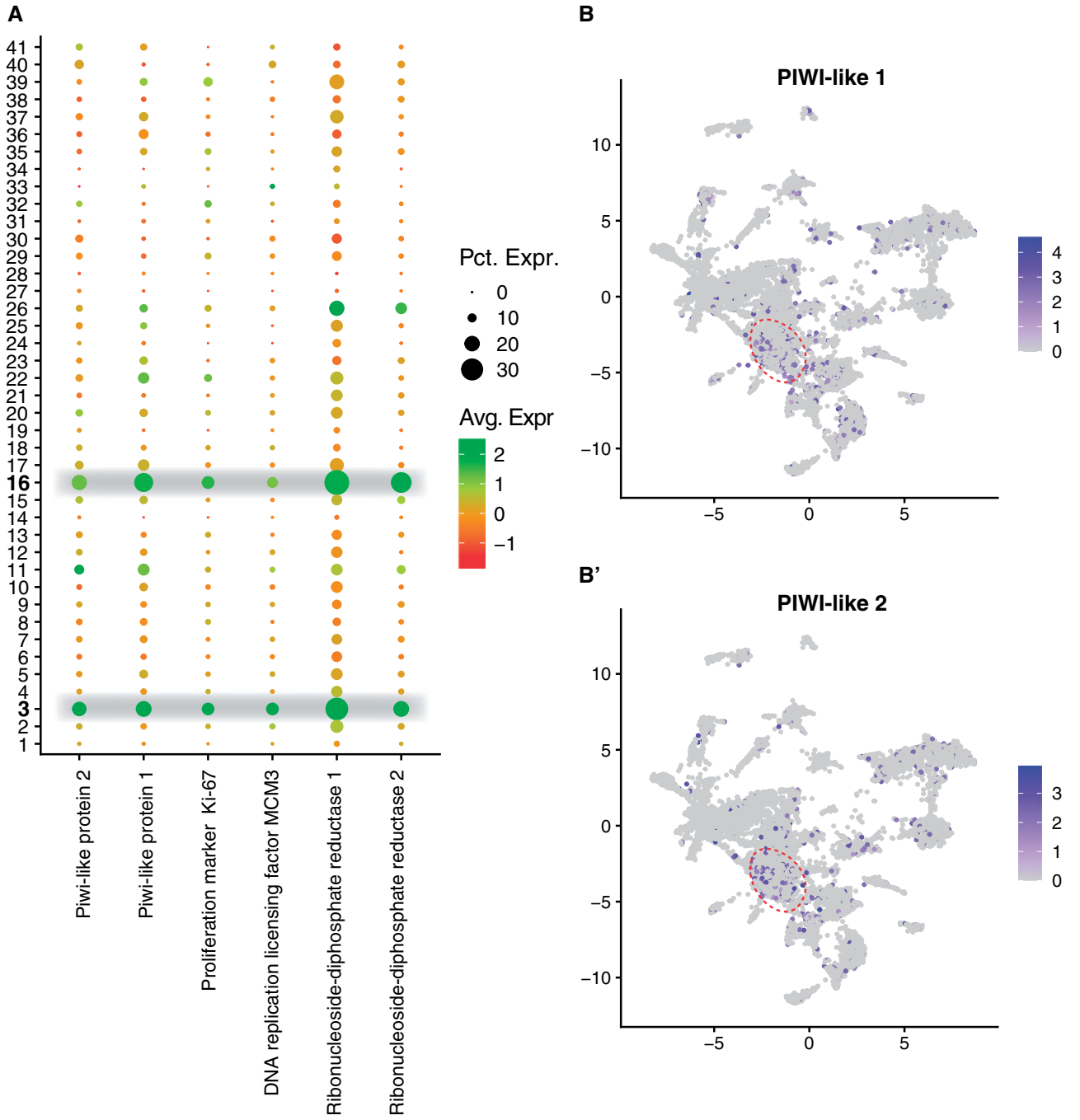

Fig. 2. Stem cells express piwi-like genes and conserved proliferation markers. (*A*) Dot plot showing expression of stem−cell and proliferation markers across all four cell clusters. (*B*) Feature plots showing the expression of *PIWI-like 1* and *PIWI-like 2* across all cells. Red-dotted line circles clusters 3 and 16.

2; those profiles are mainly aggregated in two clusters of cells (fig. 2*A* and *B*), both of which express a variety of other genes involved in proliferation, cell growth, DNA replication, organelle biosynthesis, and protein synthesis (fig. 2*A*). These two separate clusters could correspond to separate populations stem cells and germ cells accordingly with previous studies of *piwi-like* expression in hatchlings (De Mulder et al. 2009). However, the genes that are differentially expressed between these two clusters are not sufficient to discriminate these two populations. Although most of these markers are concentrated within two clusters many other cell types seem to have cells sharing an elevated expression of *piwi-like 1* and *piwi-like 2* genes (fig. 2*B*). To support our hypothesis that these cells are mostly stem cells and/or germ cells expression patterns of the proliferation marker ribonucleoside-diphosphate reductase (*rir2*) involved in DNA synthesis with single-molecule fluorescent ISH (smFISH). The expression of this gene seemed to occur in much fewer cells than previously described (De Mulder et al. 2009; supplementary fig. S5, Supplementary Material online).

Isodiametra pulchra Nervous System Displays a High Diversity of Sensory Cell Types

Because of the high number of clusters with neuronal profiles (ten clusters in total), all the cells from these clusters were batched together and subclustered using ten principal components and a resolution of 0.6 to obtain finer distinctions between neuronal subtypes. This procedure resulted in a total of 12 neuronal subclusters. The clusters were sorted into categories defined based on the expression of certain specific markers (fig. 3A). A large population of cholinergic neurons was identified based on the broad expression of *choline acetyltransferase* (Slemmon et al. 1991; Kim et al. 2006; Achatz and Martinez 2012). Presumed neuronal precursors or differentiating, immature neurons were characterized based on the expression of growth factor-related genes (*epidermal growth factor like-1*, *cd63*), DNA synthesis (*elongation factor 1A2*, *DNA primase/helicase*), and mitosis markers (*microtubule-associated proteins RP/EB*). Another cluster was characterized by the expression of several Transient Channel Potential (TRPs) orthologs (*trpc5a, trpc5b, trpc4, trpa1*), which are classically associated with sensory functions (Montell and Rubin 1989; Brauchi et al. 2006; Peng et al. 2015; Kozma et al. 2018). However, due to the absence of other clear sensory markers in these clusters, they were simply called TRP^+ neurons. The expression of *trpc5a* was assessed using a smFISH technique. We observed a clear expression domain located in the anterior tip of the animal (fig. 3C) and in the periphery of the brain. The revealed pattern indicates that some trpc5a-expressing cells are closely connected to the brain, either as a sensory input or as part of the central nervous system itself. The absence of photosensory neurons in this species has been mentioned by different authors but has never been studied in detail. In this context, we performed an additional analysis of TRP^+ neurons with the aim of looking for possible correlations between TRP and Opsin expression levels (supplementary fig. S3, Supplementary Material online). This analysis revealed that TRP^+ neurons also express more opsins than any other clusters suggesting that some of these cells could indeed be functioning as photoreceptor neurons. Additional smFISH experiments were performed to assess expression of *trpc4* and *Opsin-10*. Interestingly, the results show coexpression of these two genes in cells located on the periphery of the brain (supplementary fig. S5, Supplementary Material online).

Serotoninergic neurons were identified by the expression of a serotonin transporter (*sc6a4*) (Blakely et al. 1991; Corey et al. 1994; Chang et al. 1996). High expression of the microtubule stabilizer *saxo2* indicated that these cells are likely ciliated, which could serve a mechanosensory function. Immunostainings with antibodies against serotonin highlighted a population of serotoninergic neurons in the brain of the animal with cell bodies located toward the anterior tip (fig. 3C). These neurons display a bipolar morphology that appears to connect the tip of the animal to the CNS supporting their presumed function as sensory cells. Immunoreactivity of serotoninergic neurons has been documented in previous studies (Achatz and Martinez 2012; Dittmann et al. 2018) but was rather described as a component of the CNS and not necessarily as sensory cells. Our study shows significantly less axonal projections in the brain but the overall staining of the neuropil and cell bodies is consistent with previously published work. The juvenile animals used in our also have much fewer cells compared with the adults used in previous studies of serotoninergic neurons.

Four clusters of distinct cell populations were identified as chemosensory, based on the expression of different combinations of amiloride-sensitive sodium channels and acid-sensing sodium channels (supplementary table 2, Supplementary Material online). Chemosensory cells could be resolved into two distinct populations with one expressing predominantly glutamate receptors (*NMDA-1*, *Glr1*, *Grl2*) and the other expressing predominantly acetylcholine receptors (*AChR-1*, *AChR-2*, *AChR-3*, fig. 3A). This suggests that these sensory cells likely do not only have the ability to respond to chemical stimuli from the environment but could also to be modulated by other neurons. The detection with smFISH for *amiloride-sensitive sodium channel 1* revealed instances of expression in the proximity of the brain (fig. 3C). The expression pattern is consistent with the presumed function of these cells to sense chemical compounds in the environment during navigation.

One cluster of identified cells is possibly involved in providing nutrients to the nervous system since they express several lipoproteins receptors (*ldlr1*, *lrp2*). The function of these cells is uncertain, but they could be providing metabolic support to the nervous system in a glial cell-like manner but due to the broad expression of many lipoprotein receptors in other cell types it is not sufficient to support that hypothesis. However, since tentative glial cells have been identified already in another acoel, *S. roscoffensis* (Bery et al. 2010), this remains a plausible hypothesis.

This subclustering of cells with neuronal profiles did not show strong expression of neuropeptides and no indication of peptidergic neurons was reflected by this clustering. However, given the extensive knowledge of the repertoire of neuropeptides of *I. pulchra* provided in past studies (Thiel et al. 2018), all identified neuropeptide genes for *I. pulchra* were analyzed in our data set (supplementary data S4, Supplementary Material online). As a result, we could observe that many of them are expressed in neuronal clusters although not exclusively. Particularly striking are the neuropeptides *amidated-MIGFG-peptide* that are highly expressed in proposed chemosensory cells and *MRF-peptides* that are expressed in many TRP+ neurons (supplementary data S4A, Supplementary Material online). Some of these sequences are also expressed in proposed secretory cells and the peptide *bursicon-alpha-like* is a marker of a specific population of secretory cells (supplementary data S4B, Supplementary Material online).

Digestion and Nutrient Transport Can Be Shared within a Single-Cell Type

All clusters previously identified as digestive cells (I and II) were further analyzed. Digestive cells were characterized by the expression of various digestive enzymes such as

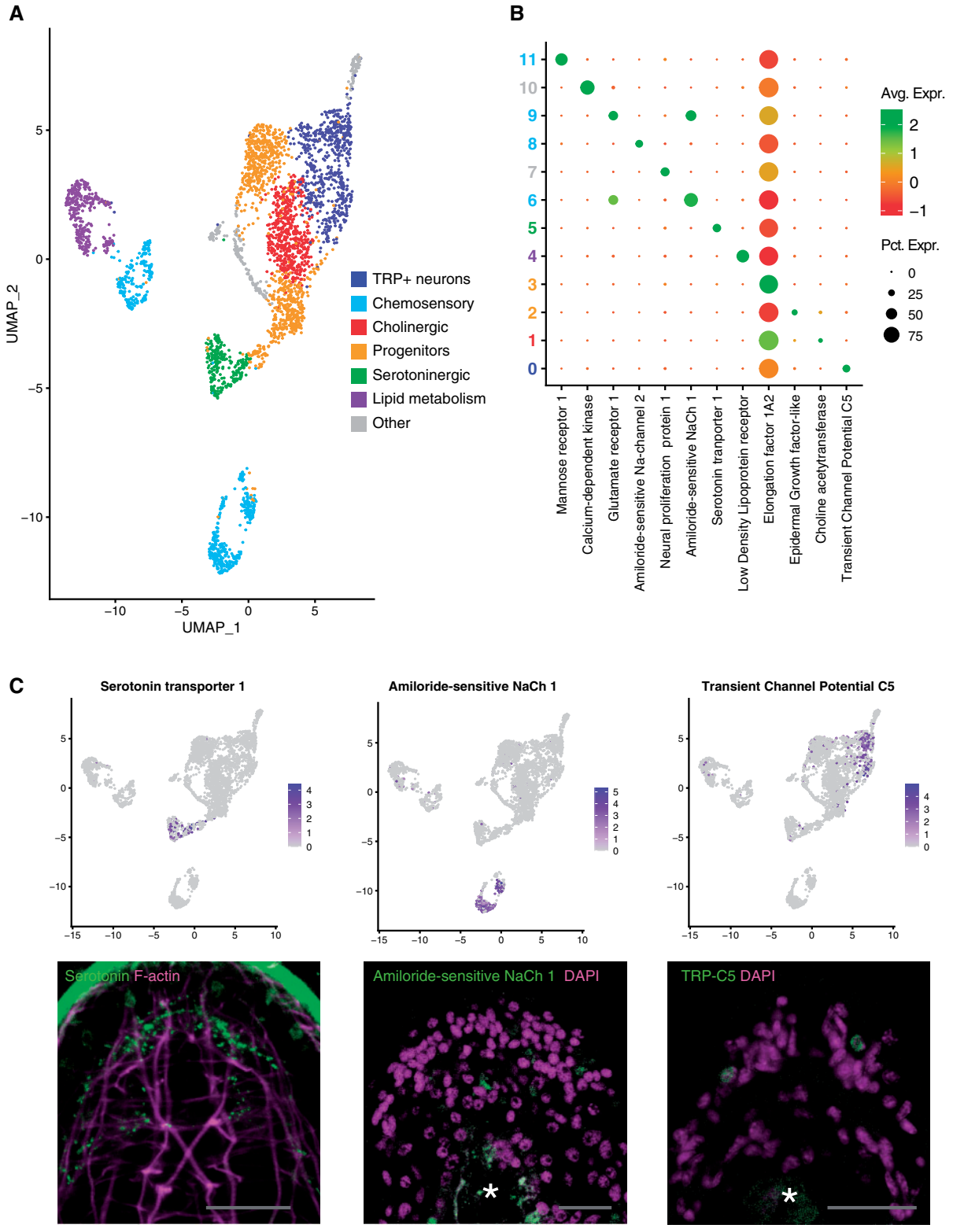

FIG. 3. Isodiametra nervous system displays a high diversity of sensory cell types. (*A*) UMAP showing neuronal subclusters and their assigned categories. (*B*) Dot plot showing the expression of main markers of each of the 12 clusters. Cluster numbers are colored according to their assigned categories. (*C*) Feature plots showing the expression of different specific neuronal markers with corresponding images showing immunostaining with antiserotonin antibody (juvenile stage) and single-molecule florescent in situ hybridization for *Amiloride-sensitive Na+ channel 1* (juvenile stage) and *trpc5* (hatchling stage). Asterisks indicate nonspecific staining in the digestive syncytium. On all images, the anterior part of the animal is shown. Scale bars = 25 μM.

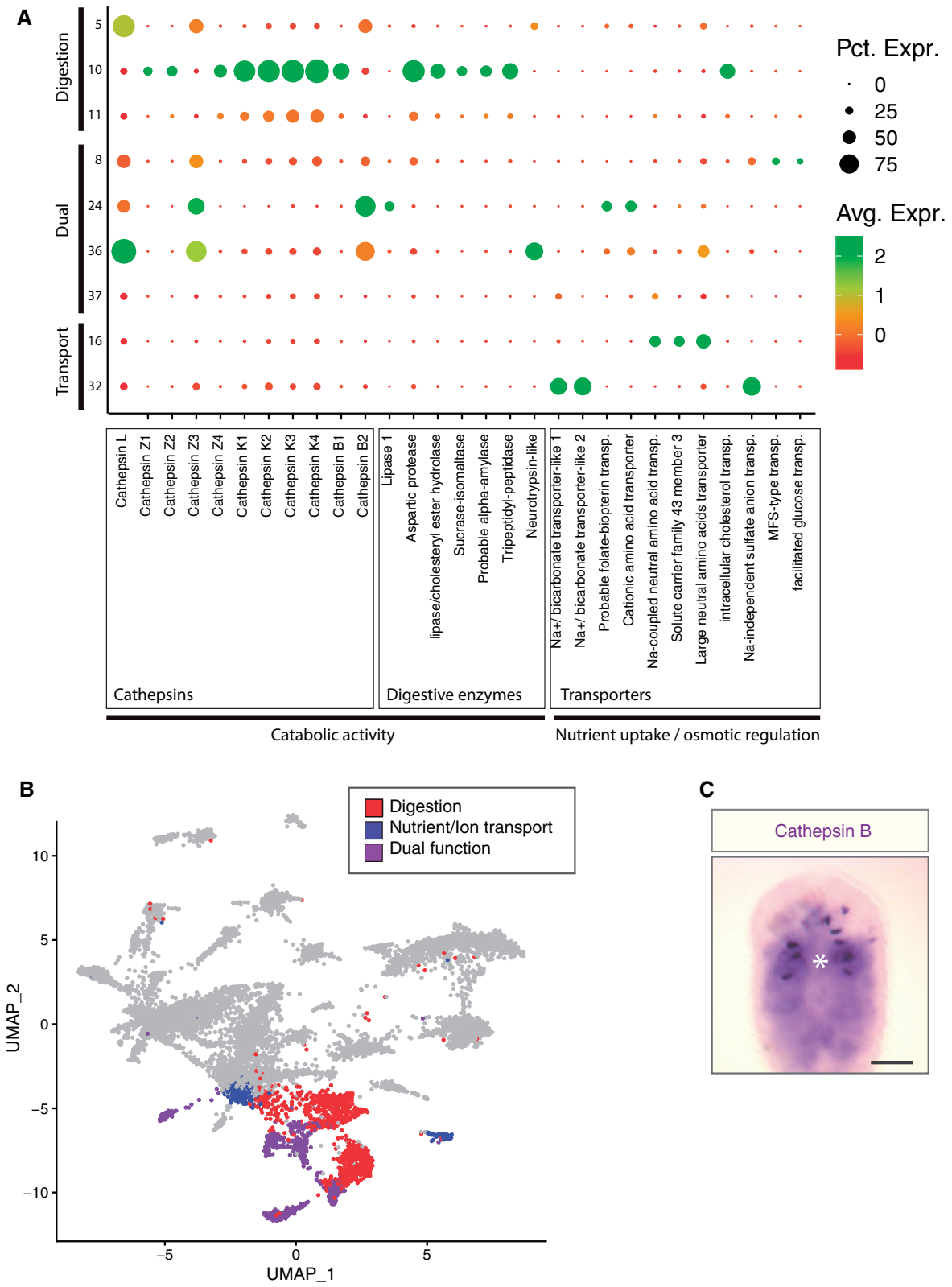

FIG. 4. Digestion and nutrient transport can be shared within a single cell type. (*A*) Dot plot showing the expression of specific markers for 9 identified as "Digestive I" and "Digestive II." Genes are sorted by functional categories. (*B*) UMAP highlighting the cell types involved in digestion, nutrient transport or both. (*C*) In situ hybridization showing the expression pattern of *cathepsin B2* (adult stage). White asterisk indicates the location of the mouth opening although it cannot be seen on this picture. Scale bar = 50 μM.

peptidases and lipases (fig. 4*A*) and interestingly by the expression of a broad variety of cathepsins known for their catabolic activity but usually inside lysosomes. Cathepsins have been previously described as markers for a novel cell

type in *Schmidtea mediterranea* (Fincher et al. 2018; Swapna et al. 2018); however, we show here with the coexpression of cathepsins and other digestive enzymes that their function in acoels is likely to be involved in the digestion of food. Whether this digestion happens through secretion of these enzymes into the digestive syncytium or intracellularly remains unknown. In the case of *I. pulchra* as well as many other acoelomorphs, digestion is supposed to be carried out by the digestive syncytium, a very large polynucleated cell capable of engulfing and digesting food (Gavilán et al. 2016); though it is unclear whether additional cells in the periphery are also involved. Our experimental procedure was designed to dissociate and isolate individual cells of up to 40 μM and therefore excluded the digestive syncytium from the experimental system. Indeed, this large structure would be excluded because of its size and morphology and could not be processed through a microfluidics-based system such as the one used in this study. Strikingly, our data show clearly that there are other cell types also contributing to the digestion of nutrients. These cells are likely to be layering the digestive syncytium to either take in food particles from the syncytium and digest them intracellularly and/or directly secrete digestive enzymes into the syncytium. This assertion is further supported by the expression pattern of *cathepsin B2* shown by ISH in cells located in the periphery anterior of the digestive syncytium (fig. 4C).

Cells expressing nutrient and ion transporters were identified (fig. 4A). These cells could be serving the function of both distributing nutrients to other cells and/or, like an excretory system, to filtrate and reabsorb necessary elements while discarding waste. The existence of such an excretory cell type in *I. pulchra* was previously proposed in Andrikou et al. (2019). We looked for the genes tested as excretory markers in that study and found high expression levels of *nephrin/kirre* and *aquaporin b* in a large population of these transporter-rich cells, consistent with their hypothesis regarding their possible excretory function.

Several clusters express a mix of digestive enzymes and transporters suggesting an ability to serve both functions of secreting digestive enzymes and taking up the processed nutrients, which suggests the presence of cellular variegated phenotypes (fig. 4A). Additional smFISH for *potassium-channel K5* specifically expressed in cluster 8, which expresses both various transporters and digestive-related genes show that these cells are located close to the posterior end of the digestive syncytium (supplementary fig. S5, Supplementary Material online). This shows that these cells are indeed likely to be involved in digestion and nutrient uptake and transport.

Acoel Epithelial and Secretory Cells Predict High Functional Diversity

Acoels only possess one epithelium that is delineating the external surface of the body unlike internal organs and tissues of most other bilaterians. This single external epithelium is known to contain many different glands and secretory cells (Achatz and Martinez 2012). For this reason and because of the shared expression of some common markers including several members of the spondin, lectin, cadherin, and fibrillin gene families, epithelial cells and secretory cells were analyzed together. Despite clear commonalities, we have observed that these cell categories are highly diversified and composed of many subtypes. These populations of cells were separated into three categories: epithelial, secretory, and motor ciliated cells, each containing several subcategories based on differential marker expression (fig. 5A and B). Epithelial cells were mainly defined by the expression of the transcript for *mucin-like*, encoding for secreted protein characteristic of epithelia in many animal species (Marin et al. 2008), and of multiple type cadherins and protocadherins responsible for cell–cell adhesion, critical for epithelium formation. These cells also expressed *sortilin-related* receptors (Mazella et al. 2019), which are broadly studied in vertebrates but are of unknown function in invertebrates. Interestingly, this cell type category expresses a *myosin-11* ortholog that could be an indicator of cell contractility. Expression of the *mucin-like* gene assessed by smFISH was observed on the outer surface of the animals consistently with the proposed epithelial identity of these cells (supplementary fig. S5, Supplementary Material online).

Secretory cells were one of the most diverse group of identified cell types in our data set. Many genes identified in these clusters had no known orthologs making it difficult to assess cell type identity, but they nevertheless shared some conserved core markers: most of these cells express at least one type of fibrillin, and/or spondin. Expression of members of the lectin and fucolectin families, as well as cysteine-rich venom-related proteins (*va5*, *vpl1*), suggest a possible involvement in defense against predators and/or pathogens. A subset of secretory cells strongly expressed an ortholog of an *adhesive plaque matrix protein*, a protein known to form a strong glue-like substance that is molded into holdfast threads in the mussel *Mytilus galloprovincialis* (Inoue and Odo 1994).

Motor ciliated cells were characterized by the very high expression of tubulins, presumably involved in motile cilia formation as well as dyneins (*Dynein heavy chain-1*, *dynein heavy chain-2*) known to be involved in the movements of cilia. Dyneins are also frequently found in other epithelial cells (fig. 5A), indicating that they might not be the only cell type with motile cilia. Additionally, the general aspect of the ciliated epithelium of *I. pulchra* can be observed with immunostainings against acetylated tubulin which reveals the density of cilia on the external epithelium of the animal (fig. 5C). Whether these proposed motor ciliated cells are used in locomotion remains however unknown. Additional smFISH experiments to check for the expression of the motor cilia-related gene *dynein heavy chain-1* revealed perinuclear expression in cells near the outer epithelium and at the very surface of the epithelium itself consistent with its presumed function in ciliated cells.

SmFISH for *adhesive plaque matrix protein* (secretory cells), *SCO-Spondin 3* (Secretory cells), and *Fucolectin-6* (Epithelial cells) showed scattered patterns of expression throughout the superficial layer of the body with slightly higher occurrence in the anterior half of the animal (fig. 5D). This suggests that secretory cells in acoels are not only grouped in specific secretory glands (Pedersen 1965; Klauser 1986) but can also

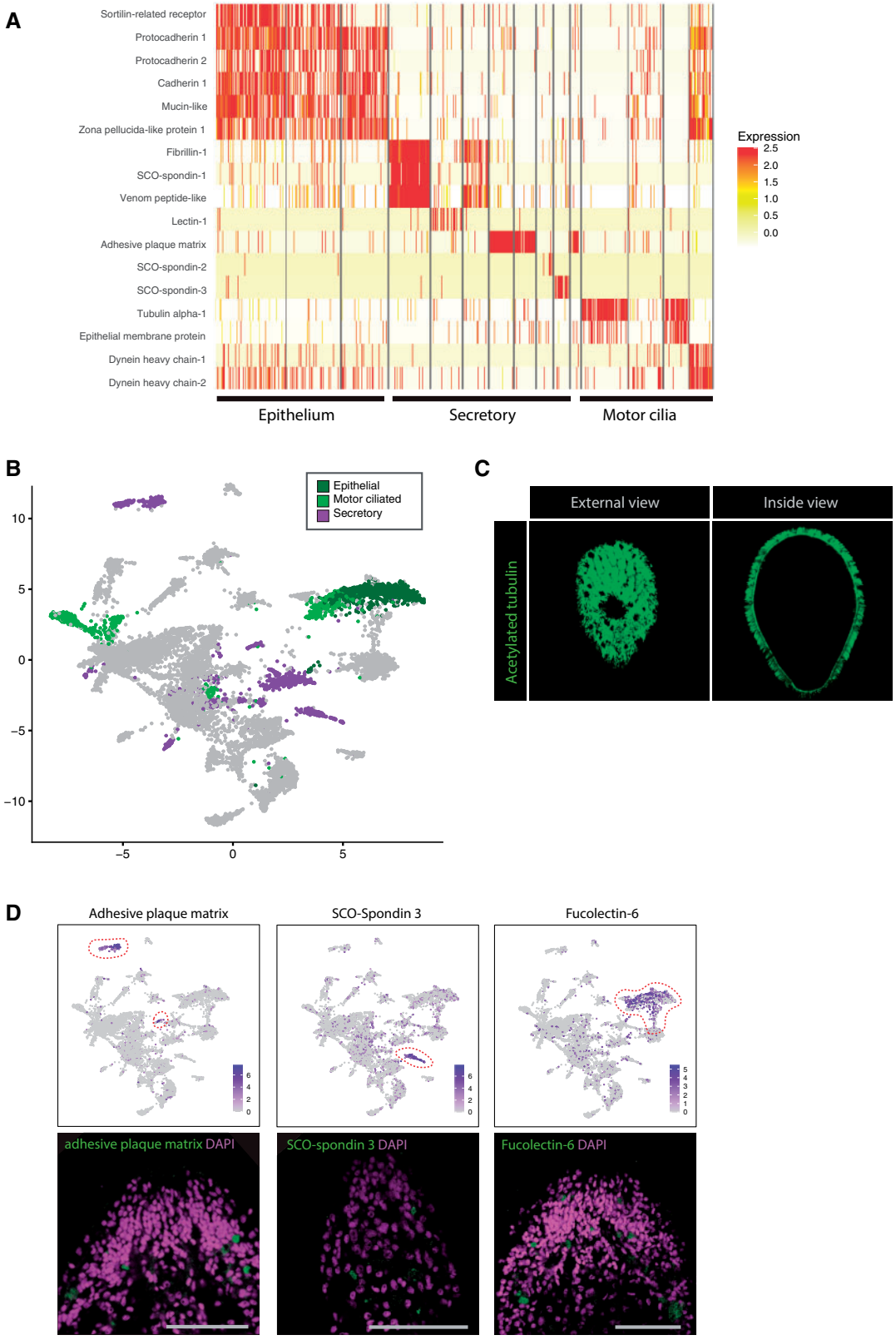

Fig. 5. Acoel epithelial and secretory cells predict high functional diversity. (*A*) Heat map showing the expression level-specific markers for the 15 cell clusters identified as "Epithelial I," "Epithelial II," and "Secretory." Rows represent genes and columns represent cells. (*B*) UMAP highlighting the cell types presumed to be epithelial, motor ciliated and or secretory. (*C*) Immunostainings using antiacetylated tubulin antibody (green) highlighting the heavy ciliation of epithelial cells of a juvenile *Isodiametra pulchra* on the ventral surface (left) and on the sides (right). The anterior part of the animal is up. Scale bars = 25 μM. (*D*) Feature plots showing the expression of the specific markers for secretory and epithelial cells *adhesive plaque matrix* (adult stage), *SCO-Spondin 3* (adult stage) and *fucolectin-6* (juvenile stage). All images show the anterior part of the animal. Scale bars = 50 μM.

be present throughout the epithelium. Additionally, the expression of the cell–cell adhesion proteins cadherins and protocadherins in some secretory cells may indicate that they use these proteins to attach to the epithelium. Based on the data collected for different types of secretory cells, it seems probable that, at least, some of these cells are involved in processes of active external secretion (i.e., mucus; Klauser 1986) or in innate defense mechanisms.

Muscle Cells Show High Marker Conservation with Other Bilaterians

Specific genes involved in the formation of contractile fibers enabled the characterization of three clusters of muscle cells (Ladurner and Rieger 2000; Rieger and Ladurner 2003; Raz et al. 2017). Major components of contractile fibers such as *myosin heavy chain*, *myosin regulatory light chain*, *troponin T*, *sarcalumenin*, and *tropomyosin* are broadly expressed in two of those clusters (fig. 6A). Interestingly, certain markers suggest similarities between muscle cells and epithelial cells. For instance, *laminin*, which is a major component of the basal lamina of epithelia appears here to be broadly expressed in muscle cells. These similarities are reflected on a UMAP plot in which the main muscle cell clusters is relatively close to epithelial cells with the consistent appearance of a smaller cluster that seems to bridge clusters of muscle and epithelial cells (fig. 6B). This latter cluster indicates the presence of a set of muscle cells that share markers with epithelial cells (*cadherin*, *protocadherin-1*, *protocadherin-2*, *and fucolectin-6*) which are mostly involved in cell–cell adhesion. This could indicate that these muscle cells are anchored to the epithelium through cadherins. Since acoels rely on the sole use of cilia of epithelial cells for locomotion it is likely that there must a close coordination between the function of the ciliated epithelium and contractile muscle to modulate movements.

Muscle cells are one of the few cell types in which defining transcription factors can be identified in our data set: The transcription factors *krueppel-like factor* and *COUP* are specifically detected in muscle clusters. In addition, the *wnt* interacting partner *frizzled* is specifically expressed in all three of these muscle clusters (fig. 6A). The whole structure muscle network of *I. pulchra* can be observed with phalloidin staining of actin filaments (fig. 6C). Additional ISH for *tropomyosin* showed high expression in or around the gonads (fig. 6C). This last result had been observed before but additional expression in all muscle was also observed (Chiodin et al. 2013), which may indicate that the staining in our ISH experiment is much weaker and only shows the cells in which *tropomyosin* expression is very high.

Interestingly, most of these presumed muscle cells also express several types of acetylcholine receptors (*AChR-4*, *AChR-5*, *AChR-6*), indicating that the neuromuscular junctions are likely mediated by cholinergic neurons (see fig. 3).

Cell Type Markers Are Conserved within the Xenacoelomorpha

In an attempt to detect the presence of both Acoela-specific and Xenacoelomorpha-specific cell types or signatures, we extracted the sequences of *I. pulchra* for which we could not identify orthologs in other clades and compared them with other transcriptomes for two other Xenacoelomorphs: *S. roscoffensis* and *X. bocki* (Brauchle et al. 2018). As a result, we identified 4,332 unknown sequences that have orthologous sequences in *S. roscoffensis* and 3,063 in *X. bocki*. We observed that all Xenacoelomorpha-specific sequences found among the cell type markers were also present in the group "Acoela-specific," with only one exception, suggesting that these genes' sequences are well conserved among Xenacoelomorpha, even though they do not have similarities with sequences of other phyla. They represent a collection of very derived sequences that could still represent orthologs of other genes but highly modified or alternatively represent Xenacoelomorpha-specific novelties. The fact that they are expressed in all three species also indicates that they are likely to be functionally relevant. We initially looked for these genes in the group of "uncharacterized" cell types but the fraction of Acoela- and Xenacoelomorpa-specific sequences in these clusters was not higher than in other clusters with assigned phenotype. This prompted us to avoid characterizing them as novel Xenacoelomorpha-specific cell types. However, the relevance of these genes should not be discounted since they are abundantly present in many of the better characterized cell types, particularly in digestive, epithelial, and secretory cells plus also in some of the sensory cell types.

To conclude, the expression of well-known orthologs of bilaterian cell markers in this data set has been sufficient to classify cell types into different functional categories. However, and surprisingly, it appears that each of these categories show significant expression of transcripts shared only within Xenacoelomorpha (clade-specific transcripts). At this point, however, we cannot rule out the possibility that *I. pulchra* have some specific cell types, though the data would better fit a model in which all cell types of Acoela show some unique transcriptional profiles different from those of the remaining bilaterians. Further analysis of the genome of *I. pulchra* as well as other members of the clade could help clarify that issue and more accurately describe gene conservation among Xenacoelomorpha and their putative relationship with those of other phyla (Guijarro-Clarke et al. 2020).

Discussion

The insights into cell type diversity through single-cell RNA sequencing experiments provide a powerful way to approach cell type evolution in a highly reproducible manner. In this study, we provide a cell atlas of the juvenile acoel *I. pulchra* that displays functionally distinct cell types. This is the first time that a high-resolution expression atlas is provided for any member of the enigmatic group Xenacoelomorpha. Although the amount of predicted cell types is consistent with what has been morphologically characterized in the past, the newly characterized subsets of cells and the specific genes expressed in each of these subsets offer valuable tools to further characterize the histology and developmental trajectories of these animals.

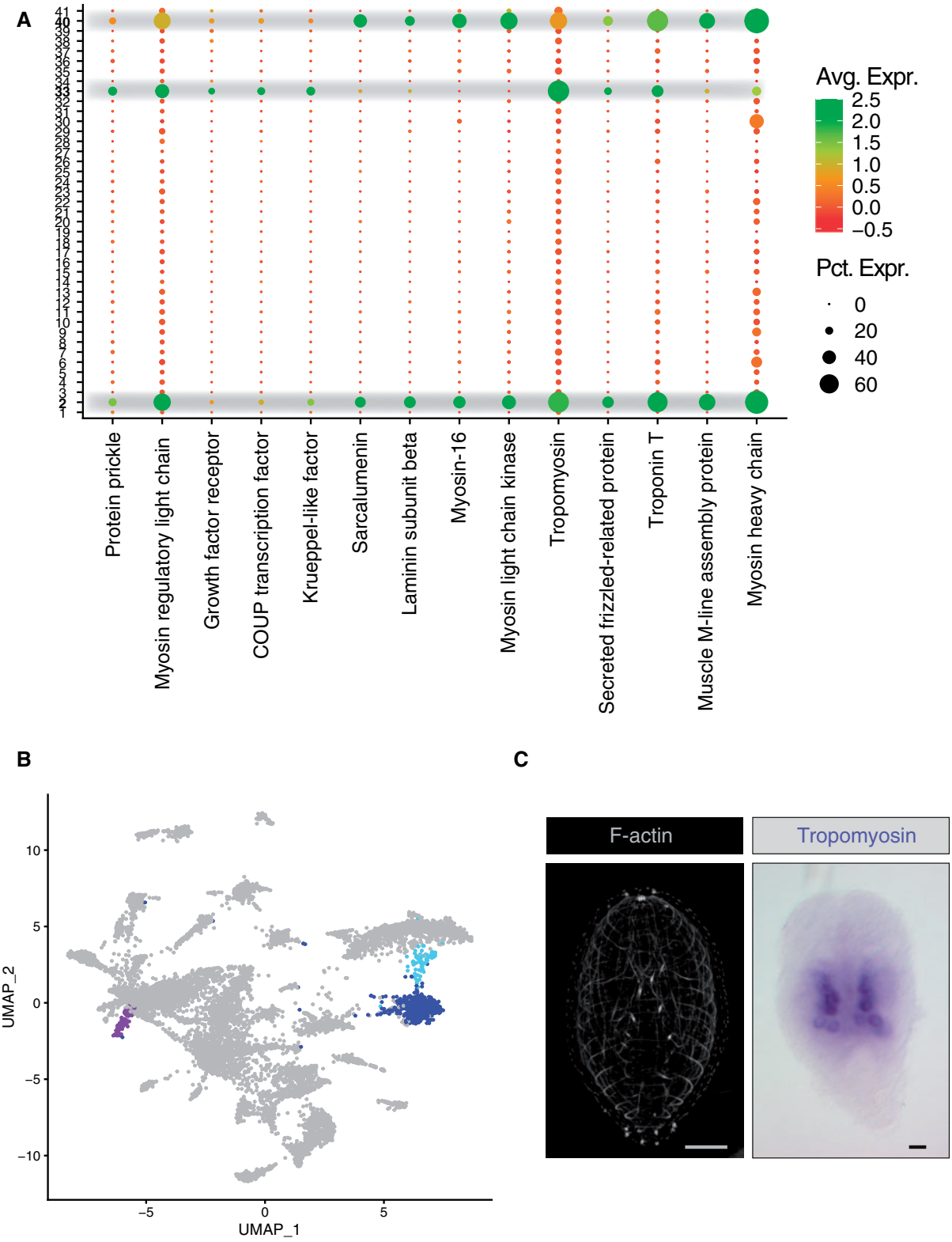

Fig. 6. Muscle cells show high marker conservation with other bilaterians. (*A*) Dot plot showing the expression of specific markers for muscle across all 41 cell clusters. Three likely candidates for muscle cells are highlighted in gray. (*B*) UMAP highlighting the three clusters identified as muscle cells. (*C*) Phalloidin staining showing the actin filament network of an *Isodiametra pulchra* juvenile (gray) and in situ hybridization for *tropomyosin*. Scale bars = 20 μM.

The nervous system of *I. pulchra* could now be described at the level of individual cells providing additional information about the chemical modalities of neurotransmission of acoel neurons. We identified distinct types of sensory cells that could be involved in chemosensation, mechanosensation, and possibly photosensation. In addition to improving our

understanding of the nervous system of acoels, this provides an entry point to functional and behavioral studies in which the described sensory markers could be stimulated or tampered with to better understand the specific role of each sensory cell type. Additionally, we performed an analysis of the neuropeptide genes found in *I. pulchra* in previous studies (Thiel et al. 2018) and confirmed that many of these peptides are indeed expressed in neuronal populations. The markers used in this analysis of the nervous system did not show significant overlap with previous studies of gene expression in *I. pulchra*. Indeed, traditional marker genes used in evolutionary developmental studies are transcription factors that are known to be key player in determining cell type identity. However, many transcription factors are expressed in low amounts and are less likely to be detected in single-cell RNA sequencing. We could however identify many other cell type markers that can be linked to different possible neuronal functions and the enormous plasticity of nervous system architectures in the Xenacoelomorpha has now a cellular reference frame for us to understand the building blocks that give rise to this great diversity.

We showed that digestion and transport of nutrients was probably carried out by a variety of cell types that secrete different digestive enzymes, including several members of the cathepsin family. These digestion processes are likely to act together with the digestive syncytium, though it remains unclear whether the enzymes are secreted into the syncytium of act as processes of intracellular digestion. This can be the case with certain types of cathepsins that are predominantly present in lysosomes in various species (Kirschke et al. 1995). The detection of several digestive enzymes opens the possibility of better understanding one of the most enigmatic tissues of Xenacoelomorpha, the gut (Gavilán et al. 2016). Other cell types were shown to express high levels of nutrient and ion-transport related transcripts, indicating a possible function in nutrient absorption and active distribution of these nutrients to other cells. In addition, one cell cluster expresses markers that have been previously proposed as having a role in excretory processes in *I. pulchra* (Andrikou et al. 2019), suggesting an involvement of these cells in the elimination of metabolic waste. Interestingly, some cell types simultaneously express markers of both digestive enzyme and nutrient/ion transport. This could indicate that these cells have dual roles (Gazizova et al. 2017) or that we have captured progenitors that later on give rise to two phenotypically distinct cell types. Since very little is known on the maturation process of the gut, both alternatives remain possible. Together, these results show for the first time that the digestive system of acoels consists of more than just a simple, homogeneous, digestive syncytium but that it encompasses many cell types that seem to assume different and distinct roles for digestion.

We provide new information about the epithelia of *I. pulchra* by describing two main categories of epithelial cells whose phenotypes suggest distinct functions. One category seems to express more classic structural elements of epithelia whereas the other express markers of motor cilia which suggests an involvement in the locomotory behavior, which in acoels relies exclusively on ciliary motion. Our data suggest that the movements of these motor cilia are mediated by axonemal dyneins known to be a major component of cellular motors in many eukaryotes including unicellular protists (King 2012). Such distinction between different types of epithelial cells had not been observed so far at the morphological level.

The presence of secretory cells and glands in different Xenacoelomorpha have been thoroughly described at the morphological level (Pedersen 1965; Klauser 1986), with mucus secretion in *S. roscoffensis* (Acoela) proposed as an aid to locomotion (Martin 1978). The morphological diversity shown in these studies predicted that there may be many different types of secretory cells could serve many different functions in organisms. However, these different functions have not been shown yet. In this study, we extended this knowledge by describing the diversity of secretory cell types at the level of gene expression, which suggest a broad variety of functions such as adhesion and defense against predators or pathogens. This first molecular description of secretory systems of an acoel provides important elements to compare secreted products such as bioadhesive proteins and toxins to those of other animals and follow their expression over evolutionary time (Tyler 1976).

The muscle cells of *I. pulchra* could be more easily identified than other cell types because of the important conservation of core muscular components such as *myosin heavy chain* and *tropomyosin*, well conserved across metazoans. Additionally, extensive study of mesodermal gene expression in *I. pulchra* (Chiodin et al. 2013) allowed us to confirm that these markers are present in muscle cells.

The peculiarity of acoel cell types compared with other bilaterians could be anticipated given the long time that the clade has evolved independently and the fast rate of nucleotide substitution that characterize their genomes. This is a group an ancient bilaterians that diversified around 500–600 Ma. This combination of old clade diversification and the fast rate evolution of their genomes may obscure the similarity of their genes with those of other animals, resulting in an added difficulty for detecting sequence similarities. However, and in spite of the contribution of these factors, our results show that instead of predicting a large number of novel cell types, *I. pulchra* displays an array of known cell types that express a combination of some conserved markers plus some clade-specific ones. Many of the latter sequences are, indeed, conserved across the different Xenacoelomorpha pointing to the presence of some specific functions carried out by conserved cell types. This shows that despite their important diversity, Xenacoelomorpha possess some clade-specific conserved genes as is the case for other phyla (Paps and Holland 2018). How these sequences contribute to the specific character of the Xenacoelomorpha cell types remains to be studied.

Together, our results pave the way for the further analysis of the different roles that these different cell types have in the morphology and physiology of acoels. Moreover, our results identified candidate markers for elusive cell populations such as multipotent stem cells or secretory cells and help us build a

molecular map of most organ systems. For the first time, we provide a thorough analysis of gene expression in acoel individual cells. The description of a catalog of cell types in *I. pulchra* should help us understand bilaterian evolution through the perspective of its cellular constituents. This is a powerful way to access to the constructional principles that guide the different morphologies of Xenacoelomorpha or any other animal, by helping to understand the diversity and arrangement of their cellular building blocks. The presence of cell types with mixed signatures and the generalized usage of clade-specific transcripts are especially relevant since they should explain the specificities of Xenacoelomorpha tissues and their functional activities. With the data provided here and the implementation of cross-species analysis of single-cell transcriptomic data, the possibility of tracing the evolutionary histories of cell types becomes a reachable objective. Single-cell data and its translation into cell type characters will be of special interest for also tracing the evolutionary history of many clades. We hypothesize that this source of data should help us, in addition, to understand the phylogenetic affinities of Xenacoelomorpha.

Materials and Methods

Animal Culture and Breeding

Isodiametra pulchra were kept in glass petri dishes at 20 °C. *Nitzschia curvilineata* diatoms were transferred from an agar stock to petri dishes containing F/2 medium (Guillard and Ryther 1962) and were grown at 20 °C for a minimum of two weeks to obtain a dense biofilm at the bottom of the dish. Water was then changed to artificial seawater with a salinity of 32ppt and *I. pulchra* were added in the dish. Animals were kept for up to six weeks in the same dish before being transferred to a dish with freshly grown diatoms.

Transcriptome Processing and Annotation

All transcriptomes used in this study were previously published in Brauchle et al. (2018). The transcriptome of *I. pulchra* was further processed and redundancy of sequences was reduced using Corset (Davidson and Oshlack 2014). The number of transcripts could therefore be reduced from 320,563 to 45,515 sequences. Completeness of the transcriptome was assessed with Benchmarking Universal Single-Copy Orthologs (BUSCO version 3.0.2, Simão et al. 2015; Seppey et al. 2019). Functional annotation of the nonredundant transcriptome was performed by searching for sequence homology between *I. pulchra* transcripts and subsequent protein sequence predictions to the *Swissprot* protein database as well as the *Pfam* database of protein families using BlastX (version 2.7.1).

Single-Cell Dissociation

A hundred *I. pulchra* hatchlings were used for each single-cell RNA sequencing experiment. Animals were dissociated for 1 h at 25 °C in a collagenase solution (Sigma–Aldrich C9722) at a concentration of 1 mg/ml in RNAse-free phosphate buffer (PBS) in 2-ml plastic tubes under continuous agitation. The suspension was then centrifuged for 5 min at 750rcf and the resulting pellet was resuspended in RNAse-free PBS with 0.4% bovine serum albumin (Thermo Fischer Scientific AM2616). Cells were then filtered through a 40-μM *Flowmi* Cell strainer (Bel-Art H13680-0040). The suspension was again centrifuged for 5 min at 750rcf and the pellet was resuspended in RNAse-free PBS. The suspension was then gently pipetted up and down ∼200 times using RNAse-free pipette tips. Cell concentration was estimated by manually counting cells in a hemocytometer (Neubauer improved—Optik Labor).

Single-Cell RNA Sequencing

Two separate single-cell RNA experiments (ScRNA-Seq) were performed and the resulting single-cell sequencings were later batched together. Cell counting and viability assessments were conducted using a DeNovix CellDrop Automated Cell Counter with an Acridine Orange (AO)/Propidium Iodide (PI) assay. Gel beads emulsion (GEM) generation and barcoding, reverse transcription, cDNA amplification, and 3′ Gene Expression library generation steps were all performed according to the Chromium Single Cell 3′ reagent kits (version 3) user Guide (10× Genomics CG000183 Rev B). Specifically, 37.3 μl of each cell suspensions (300 cells/μl) were used for a targeted cell recovery of 7,000 cells. GEM generation was followed by a GEM-reverse transcription incubation, a washing step, and 12 cycles of cDNA amplification. The resulting cDNA was evaluated for quantity and quality using fluorometry and capillary electrophoresis, respectively. The cDNA libraries were pooled and sequenced paired-end and single indexed on an Illumina NovaSeq 6000 sequencer with a shared NovaSeq 6000 S2 Reagent Kit. The read setup was as follows: read 1: 28 cycles, i7 index: 8 cycles, i5: 0 cycles, and read 2: 91 cycles. An average of 521,045,087 reads/library was obtained, equating to an average of 65,130 reads/cell. All steps were performed at the Next Generation Sequencing Platform, University of Bern.

Data Processing

The reads obtained from single-cell RNA sequencing experiments were mapped to the concatenated nonredundant transcriptome of *I. pulchra* with Cell Ranger (Version 3.0.2, 10× Genomics). Integration of the data sets from the two different experiments was performed with the provided *aggregate* function of Cell Ranger. This resulted in a total of 14,864 cells with a median of 405 genes/cell.

Data Clustering and Analysis

The count matrix containing the expression level of each detected gene for each cell was analyzed with Seurat (Version 3.1.4, Satija et al. 2015; Butler et al. 2018). In order to exclude cells of poor quality and possible remaining multiplets, the data were filtered to only include cells expressing between 200 and 2,000 genes. The data were then log-normalized with a scale factor of 10,000. The 2,000 genes with the highest variability across the data set were identified with the provided *FindVariableFeatures* function with low and high cutoffs of 0.0125 and 3, respectively and a Y cutoff of 0.5. Linear transformation was then applied with the

ScaleData function. Linear dimensional reduction was performed through principal component analysis. The 25 principal components responsible for the most variability in the data were manually selected based on the assessment of an elbow plot. Clustering of the cells was performed using the *FindNeighbors* function using the 25 selected principal components and *FindClusters* function was used with the Louvain algorithm at a resolution of 2.5. Nonlinear dimensional reduction was performed to represent the data in a 2D space using Uniform Manifold Approximation and Projection (UMAP).

Immunohistochemistry

Whole animals were fixed for 30 min in a 3.7% formaldehyde solution. Primary antibodies were used at different concentrations: polyclonal 5HT antibody produced in rabbit (Sigma) 1:200; monoclonal dSAP-47 antibody produced in mouse (Developmental Studies Hybridoma Bank) 1:20, monoclonal acetylated tubulin antibody produces in mouse (Sigma) 1:500. Primary antibodies were incubated at 4 °C overnight and washed three to five times for 20 min at room temperature in phosphate buffer with 0.3% triton (PBT) secondary antibodies were added at a dilution of 1:200 together with phalloidin (1:5,000) and DAPI (1:2,000) in PBT and incubated for 2 h at room temperature. Secondary antibodies were washed at least five times for 20 min in PBT and specimens were then transferred in vectashield mounting medium (Vector laboratories) and incubated overnight at 4 °C. Specimens were mounted on microscope slides in vectashield and covered with 130–170 μM glass coverslips.

In Situ Hybridization

Animals of all stages were collected and relaxed in a 7% $MgCl_2$ solution. Samples were fixed for 30 min at room temperature in a 3.7% formaldehyde in PBT (0.3% Triton). Samples were dehydrated in 100% methanol and were stored at −20 °C. Probe synthesis and ISH were performed following a protocol designed for the planarian *Macrostomum ligano* (Pfister et al. 2007) with the following modifications: heat fixation was not performed and proteinase-K permeabilization was done for a reduced period of 8 min. Working concentration of the riboprobes was of 0.2 ng/µl. The primers used for generating the antisense riboprobes for *cathepsinB2* and *tropomyosin* with reverse transcription polymerase chain reaction (RT–PCR) are provided here.

Gene ID	Gene Name	Forward Primer	Reverse Primer
TRINITY_DN30349_c0_g4	Tropomyosin	TTGACCTCCA CCGACTTC	CCCTCTTTCCT CTACATCTCC
TRINITY_DN23833_c0_g5	Cathepsin B2	CCGCACGAGA TACAACAG	TGGGAAGCAG GGGAGAACT

Single-Molecule Fluorescent In Situ Hybridization

Sets of 48 probes of 20 bp to 22 bp were designed for each target mRNA were designed and were then synthetized with Stellaris (LGC Biosearch technologies). Animals were fixed for 1 h in 3.7% formaldehyde at room temperature and subsequently washed with phosphate buffer (PBS) before being transferred in 100% methanol to be stored at −20 °C. Specimens were rehydrated in 1:3, 2:3, and 1:1 PBT (Triton 0.3%). ISH was done following the provided protocol for Drosophila embryos (Orjalo and Johansson 2016). The hybridization temperature was increased to 45 °C overnight and the reaction volumes for hybridization were reduced to 100 μl per probe mix.

Imaging and Image Processing

All fluorescent imaging was performed on a Leica SP5 laser scanning confocal microscope using either 63× or 20× objectives. Images were treated and adjusted with Fiji. Levels were adjusted to optimize contrast of the structures of interest. Consequently, the images displayed in this paper are not adapted for quantitative analysis. An estimation of the number of cells present in nuclei was performed on an entire confocal stack of *I. pulchra* hatchlings stained with DAPI using the Imaris software (Oxford intruments) with the provided spot detection tool. The estimated spot size to detect nuclei was set at 3 μM.

Supplementary Material

Supplementary data are available at *Molecular Biology and Evolution* online.

Acknowledgments

We thank Dr Pamela Nicholson and her team at the next-generation sequencing facility (NGS) of the University of Bern for their expertise and their help with the single-cell RNA transcriptomics experiments. This work was supported by the Swiss National Science Foundation to SGS (Grant Nos. IZCOZ0_182957 and 310030_188471) and by the Agencia Estatal de Investigación to PM (Grant No. PGC2018-094173-B-I00).

Data Availability

Raw data, processed data sets for single-cell transcriptomics as well the nonredundant transcriptome used for annotation and used as reference for all single-cell RNA sequencing analysis are available on Gene Expression Omnibus (GEO) provided by NCBI (accession number GSE154049).

References

Achatz JG, Martinez P. 2012. The nervous system of *Isodiametra pulchra* (Acoela) with a discussion on the neuroanatomy of the *Xenacoelomorpha* and its evolutionary implications. *Front Zool.* 9(1):27.

Achim K, Eling N, Vergara HM, Bertucci PY, Musser J, Vopalensky P, Brunet T, Collier P, Benes V, Marioni JC, et al. 2018. Whole-body single-cell sequencing reveals transcriptional domains in the annelid larval body. *Mol Biol Evol.* 35(5):1047–1062.

Andrikou C, Thiel D, Ruiz-Santiesteban JA, Hejnol A. 2019. Active mode of excretion across digestive tissues predates the origin of excretory organs. *PLoS Biol.* 17(7):e3000408.

Arboleda E, Hartenstein V, Martinez P, Reichert H, Sen S, Sprecher S, Bailly X. 2018. An emerging system to study photosymbiosis, brain

regeneration, chronobiology, and behavior: the marine acoel *Symsagittifera roscoffensis*. *Bioessays* 40(10):e1800107.
Baguñà J, Martinez P, Paps J, Riutort M. 2008. Back in time: a new systematic proposal for the Bilateria. *Philos Trans R Soc B*. 363(1496):1481–1491.
Baguñà J, Riutort M. 2004. The dawn of bilaterian animals: the case of acoelomorph flatworms. *Bioessays*. 26(10):1046–1057.
Bailly X, Laguerre L, Correc G, Dupont S, Kurth T, Pfannkuchen A, Entzeroth R, Probert I, Vinogradov S, Lechauve C, et al. 2014. The chimerical and multifaceted marine acoel *Symsagittifera roscoffensis*: from photosymbiosis to brain regeneration. *Front Microbiol*. 5:498.
Bery A, Cardona A, Martinez P, Hartenstein V. 2010. Structure of the central nervous system of a juvenile acoel, *Symsagittifera roscoffensis*. *Dev Genes Evol*. 220(3–4):61–76.
Blakely RD, Berson HE, Fremeau RTJ, Caron MG, Peek MM, Prince HK, Bradley CC. 1991. Cloning and expression of a functional serotonin transporter from rat brain. *Nature* 354(6348):66–70.
Brauchi S, Orta G, Salazar M, Rosenmann E, Latorre R. 2006. A hot-sensing cold receptor: c-terminal domain determines thermosensation in transient receptor potential channels. *J Neurosci*. 26(18):4835–4840.
Brauchle M, Bilican A, Eyer C, Bailly X, Martínez P, Ladurner P, Bruggmann R, Sprecher SG. 2018. *Xenacoelomorpha* survey reveals that all 11 animal homeobox gene classes were present in the first bilaterians. *Genome Biol Evol*. 10(9):2205–2217.
Bryant DM, Johnson K, DiTommaso T, Tickle T, Couger MB, Payzin-Dogru D, Lee TJ, Leigh ND, Kuo T-H, Davis FG, et al. 2017. A tissue-mapped Axolotl de novo transcriptome enables identification of limb regeneration factors. *Cell Rep*. 18(3):762–776.
Butler A, Hoffman P, Smibert P, Papalexi E, Satija R. 2018. Integrating single-cell transcriptomic data across different conditions, technologies, and species. *Nat Biotechnol*. 36(5):411–420.
Cannon JT, Vellutini BC, Smith J III, Ronquist F, Jondelius U, Hejnol A. 2016. Xenacoelomorpha is the sister group to Nephrozoa. *Nature* 530(7588):89–93.
Chang AS, Chang SM, Starnes DM, Schroeter S, Bauman AL, Blakely RD. 1996. Cloning and expression of the mouse serotonin transporter. *Brain Res Mol Brain Res*. 43(1–2):185–192.
Chiodin M, Borve A, Berezikov E, Ladurner P, Martinez P, Hejnol A. 2013. Mesodermal gene expression in the acoel *Isodiametra pulchra* indicates a low number of mesodermal cell types and the endomesodermal origin of the gonads. *PLoS One* 8(2):e55499.
Corey JL, Quick MW, Davidson N, Lester HA, Guastella J. 1994. A cocaine-sensitive Drosophila serotonin transporter: cloning, expression, and electrophysiological characterization. *Proc Natl Acad Sci U S A*. 91(3):1188–1192.
Davidson NM, Oshlack A. 2014. Corset: enabling differential gene expression analysis for de novo assembled transcriptomes. *Genome Biol*. 15(7):410.
De Mulder K, Kuales G, Pfister D, Willems M, Egger B, Salvenmoser W, Thaler M, Gorny A-K, Hrouda M, Borgonie G, et al. 2009. Characterization of the stem cell system of the acoel *Isodiametra pulchra*. *BMC Dev Biol*. 9(1):69.
Dittmann IL, Zauchner T, Nevard LM, Telford MJ, Egger B. 2018. SALMFamide2 and serotonin immunoreactivity in the nervous system of some acoels (Xenacoelomorpha). *J Morphol*. 279(5):589–597.
Dupont S, Moya A, Bailly X. 2012. Stable photosymbiotic relationship under CO(2)-induced acidification in the acoel worm *Symsagittifera roscoffensis*. *PLoS One* 7(1):e29568.
Fincher CT, Wurtzel O, de Hoog T, Kravarik KM, Reddien PW. 2018. Cell type transcriptome atlas for the planarian *Schmidtea mediterranea*. *Science* 360(6391):eaaq1736.
Gavilán B, Perea-Atienza E, Martínez P. 2016. Xenacoelomorpha: a case of independent nervous system centralization? *Philos Trans R Soc B*. 371(1685):20150039.
Gazizova G, Zabotin Y, Golubev AI. 2017. Comparative morphology of parenchymal cells in Acoelomorpha and Plathelminthes. *Invertbr Zool*. 14(1):21–26.
Gehrke AR, Neverett E, Luo Y-J, Brandt A, Ricci L, Hulett RE, Gompers A, Ruby JG, Rokhsar DS, Reddien PW, et al. 2019. Acoel genome reveals the regulatory landscape of whole-body regeneration. *Science* 363(6432):eaau6173.
Guijarro-Clarke C, Holland PWH, Paps J. 2020. Widespread patterns of gene loss in the evolution of the animal kingdom. *Nat Ecol Evol*. 4(4):519–523.
Guillard RR, Ryther JH. 1962. Studies of marine planktonic diatoms. I. *Cyclotella nana* Hustedt, and *Detonula confervacea* (cleve) Gran. *Can J Microbiol*. 8(2):229–239.
Han X, Wang R, Zhou Y, Fei L, Sun H, Lai S, Saadatpour A, Zhou Z, Chen H, Ye F, et al. 2018. Mapping the mouse cell atlas by microwell-seq. *Cell* 172(5):1091–1107.e17.
Hejnol A, Martindale MQ. 2008a. Acoel development supports a simple planula-like urbilaterian. *Philos Trans R Soc B*. 363(1496):1493–1501.
Hejnol A, Martindale MQ. 2008b. Acoel development indicates the independent evolution of the bilaterian mouth and anus. *Nature* 456(7220):382–386.
Hejnol A, Martindale MQ. 2009. Coordinated spatial and temporal expression of Hox genes during embryogenesis in the acoel *Convolutriloba longifissura*. *BMC Biol*. 7(1):65.
Hulett RE, Potter D, Srivastava M. 2020. Neural architecture and regeneration in the acoel *Hofstenia miamia*. *Proc R Soc B*. 287(1931):20201198.
Inoue K, Odo S. 1994. The adhesive protein cDNA of *Mytilus galloprovincialis* encodes decapeptide repeats but no hexapeptide motif. *Biol Bull*. 186(3):349–355.
Jondelius U, Wallberg A, Hooge M, Raikova OI. 2011. How the worm got its pharynx: phylogeny, classification and Bayesian assessment of character evolution in Acoela. *Syst Biol*. 60(6):845–871.
Kapli P, Yang Z, Telford MJ. 2020. Phylogenetic tree building in the genomic age. *Nat Rev Genet*. 21(7):428–444.
Karaiskos N, Wahle P, Alles J, Boltengagen A, Ayoub S, Kipar C, Kocks C, Rajewsky N, Zinzen RP. 2017. The *Drosophila* embryo at single-cell transcriptome resolution. *Science* 358(6360):194–199.
Kim A-R, Rylett RJ, Shilton BH. 2006. Substrate binding and catalytic mechanism of human choline acetyltransferase. *Biochemistry* 45(49):14621–14631.
King SM. 2012. Integrated control of axonemal dynein AAA(+) motors. *J Struct Biol*. 179(2):222–228.
Kirschke H, Barrett AJ, Rawlings ND. 1995. Proteinases 1: lysosomal cysteine proteinases. *Protein Profile*. 2(14):1581–1643.
Klauser MD. 1986. Mucous secretions of the acoel turbellarian *Convoluta* sp. Ørsted: an ecological and functional approach. *J Exp Mar Biol Ecol*. 97(2):123–133.
Kozma MT, Schmidt M, Ngo-Vu H, Sparks SD, Senatore A, Derby CD. 2018. Chemoreceptor proteins in the Caribbean spiny lobster, *Panulirus argus*: expression of ionotropic receptors, gustatory receptors, and TRP channels in two chemosensory organs and brain. *PLoS One* 13(9):e0203935.
Ladurner P, Rieger R. 2000. Embryonic muscle development of *Convoluta pulchra* (Turbellaria-acoelomorpha, platyhelminthes). *Dev Biol*. 222(2):359–375.
Marin F, Luquet G, Marie B, Medakovic D. 2008. Molluscan shell proteins: primary structure, origin, and evolution. *Curr Top Dev Biol*. 80:209–276.
Martin GG. 1978. A new function of rhabdites: Mucus production for ciliary gliding. *Zoomorphologie* 91(3):235–248.
Martindale MQ, Hejnol A. 2009. A developmental perspective: changes in the position of the blastopore during bilaterian evolution. *Dev Cell*. 17(2):162–174.
Martín-Durán JM, Pang K, Børve A, Lê HS, Furu A, Cannon JT, Jondelius U, Hejnol A. 2018. Convergent evolution of bilaterian nerve cords. *Nature* 553(7686):45–50.
Martínez P, Hartenstein V, Sprecher S. 2017. Xenacoelomorpha Nervous Systems. In: Murray Sherman S, editor. Oxford Research Encyclopedia of Neuroscience. New York: Oxford University Press.
Mazella J, Borsotto M, Heurteaux C. 2019. Editorial: sortilin and sortilin partners in physiology and pathologies. *Front Pharmacol*. 10:791.

Montell C, Rubin GM. 1989. Molecular characterization of the *Drosophila* trp locus: a putative integral membrane protein required for phototransduction. *Neuron* 2(4):1313–1323.

Moreno E, De Mulder K, Salvenmoser W, Ladurner P, Martínez P. 2010. Inferring the ancestral function of the posterior Hox gene within the bilateria: controlling the maintenance of reproductive structures, the musculature and the nervous system in the acoel flatworm *Isodiametra pulchra*. *Evol Dev*. 12(3):258–266.

Moreno E, Nadal M, Baguna J, Martinez P. 2009. Tracking the origins of the bilaterian Hox patterning system: insights from the acoel flatworm *Symsagittifera roscoffensis*. *Evol Dev*. 11(5):574–581.

Nissen M, Shcherbakov D, Heyer A, Brummer F, Schill RO. 2015. Behaviour of the plathelminth *Symsagittifera roscoffensis* under different light conditions and the consequences for the symbiotic algae *Tetraselmis convolutae*. *J Exp Biol*. 218(11):1693–1698.

Orjalo AVJ, Johansson HE. 2016. Stellaris(R) RNA fluorescence in situ hybridization for the simultaneous detection of immature and mature long noncoding RNAs in adherent cells. *Methods Mol Biol*. 1402:119–134.

Packer JS, Zhu Q, Huynh C, Sivaramakrishnan P, Preston E, Dueck H, Stefanik D, Tan K, Trapnell C, Kim J, et al. 2019. A lineage-resolved molecular atlas of *C. elegans* embryogenesis at single-cell resolution. *Science* 365(6459):eaax1971.

Paps J, Holland PWH. 2018. Reconstruction of the ancestral metazoan genome reveals an increase in genomic novelty. *Nat Commun*. 9(1):1730.

Pedersen KJ. 1965. Cytological and cytochemical observations on the mucous gland cells of an acoel turbellarian, *Convoluta convulta*. *Ann N Y Acad Sci*. 118(24):930–965.

Peng G, Shi X, Kadowaki T. 2015. Evolution of TRP channels inferred by their classification in diverse animal species. *Mol Phylogenet Evol*. 84:145–157.

Perea-Atienza E, Botta M, Salvenmoser W, Gschwentner R, Egger B, Kristof A, Martinez P, Achatz JG. 2013. Posterior regeneration in *Isodiametra pulchra* (Acoela, Acoelomorpha). *Front Zool*. 10(1):64.

Perea-Atienza E, Sprecher SG, Martinez P. 2018. Characterization of the bHLH family of transcriptional regulators in the acoel *S. roscoffensis* and their putative role in neurogenesis. *Evodevo* 9(1):8.

Pfister D, De Mulder K, Philipp I, Kuales G, Hrouda M, Eichberger P, Borgonie G, Hartenstein V, Ladurner P. 2007. The exceptional stem cell system of *Macrostomum lignano*: screening for gene expression and studying cell proliferation by hydroxyurea treatment and irradiation. *Front Zool*. 4(1):9.

Philippe H, Brinkmann H, Copley RR, Moroz LL, Nakano H, Poustka AJ, Wallberg A, Peterson KJ, Telford MJ. 2011. Acoelomorph flatworms are deuterostomes related to *Xenoturbella*. *Nature* 470(7333):255–258.

Philippe H, Poustka AJ, Chiodin M, Hoff KJ, Dessimoz C, Tomiczek B, Schiffer PH, Muller S, Domman D, Horn M, et al. 2019. Mitigating anticipated effects of systematic errors supports sister-group relationship between Xenacoelomorpha and Ambulacraria. *Curr Biol*. 29(11):1818–1826.e6.

Plass M, Solana J, Wolf FA, Ayoub S, Misios A, Glažar P, Obermayer B, Theis FJ, Kocks C, Rajewsky N. 2018. Cell type atlas and lineage tree of a whole complex animal by single-cell transcriptomics. *Science* 360(6391):eaaq1723.

Raikova OI, Reuter M, Jondelius U, Gustafsson MKS. 2000. An immunocytochemical and ultrastructural study of the nervous and muscular systems of *Xenoturbella westbladi* (Bilateria inc. sed.). *Zoomorphology* 120(2):107–118.

Raz AA, Srivastava M, Salvamoser R, Reddien PW. 2017. Acoel regeneration mechanisms indicate an ancient role for muscle in regenerative patterning. *Nat Commun*. 8(1):1260.

Rieger RM, Ladurner P. 2003. The significance of muscle cells for the origin of mesoderm in bilateria. *Integr Comp Biol*. 43(1):47–54.

Robertson HE, Lapraz F, Egger B, Telford MJ, Schiffer PH. 2017. The mitochondrial genomes of the acoelomorph worms *Paratomella rubra*, *Isodiametra pulchra* and *Archaphanostoma ylvae*. *Sci Rep*. 7(1):1847.

Ruiz-Trillo I, Riutort M, Littlewood DT, Herniou EA, Baguña J. 1999. Acoel flatworms: earliest extant bilaterian Metazoans, not members of Platyhelminthes. *Science* 283(5409):1919–1923.

Satija R, Farrell JA, Gennert D, Schier AF, Regev A. 2015. Spatial reconstruction of single-cell gene expression data. *Nat Biotechnol*. 33(5):495–502.

Sebe-Pedros A, Chomsky E, Pang K, Lara-Astiaso D, Gaiti F, Mukamel Z, Amit I, Hejnol A, Degnan BM, Tanay A. 2018. Early metazoan cell type diversity and the evolution of multicellular gene regulation. *Nat Ecol Evol*. 2(7):1176–1188.

Sebe-Pedros A, Saudemont B, Chomsky E, Plessier F, Mailhe M-P, Renno J, Loe-Mie Y, Lifshitz A, Mukamel Z, Schmutz S, et al. 2018. Cnidarian cell type diversity and regulation revealed by whole-organism single-cell RNA-seq. *Cell* 173(6):1520–1534.e20.

Semmler H, Chiodin M, Bailly X, Martinez P, Wanninger A. 2010. Steps towards a centralized nervous system in basal bilaterians: insights from neurogenesis of the acoel *Symsagittifera roscoffensis*. *Dev Growth Differ*. 52(8):701–713.

Seppey M, Manni M, Zdobnov EM. 2019. BUSCO: assessing genome assembly and annotation completeness. *Methods Mol Biol*. 1962:227–245.

Siebert S, Farrell JA, Cazet JF, Abeykoon Y, Primack AS, Schnitzler CE, Juliano CE. 2019. Stem cell differentiation trajectories in Hydra resolved at single-cell resolution. *Science* 365(6451):eaav9314.

Simão FA, Waterhouse RM, Ioannidis P, Kriventseva EV, Zdobnov EM. 2015. BUSCO: assessing genome assembly and annotation completeness with single-copy orthologs. *Bioinformatics* 31(19):3210–3212.

Slemmon JR, Campbell GA, Selski DJ, Bramson HN. 1991. The amino terminus of the putative Drosophila choline acetyltransferase precursor is cleaved to yield the 67 kDa enzyme. *Brain Res Mol Brain Res*. 9(3):245–252.

Smith JPS III, Bush L. 1991. *Convoluta pulchra* n. sp. (Turbellaria: Acoela) from the East Coast of North America. *Trans Am Microsc Soc*. 110(1):12–26.

Sprecher SG, Bernardo-Garcia FJ, van Giesen L, Hartenstein V, Reichert H, Neves R, Bailly X, Martinez P, Brauchle M. 2015. Functional brain regeneration in the acoel worm *Symsagittifera roscoffensis*. *Biol Open*. 4(12):1688–1695.

Srivastava M, Mazza-Curll KL, van Wolfswinkel JC, Reddien PW. 2014. Whole-body acoel regeneration is controlled by Wnt and Bmp-Admp signaling. *Curr Biol*. 24(10):1107–1113.

Swapna LS, Molinaro AM, Lindsay-Mosher N, Pearson BJ, Parkinson J. 2018. Comparative transcriptomic analyses and single-cell RNA sequencing of the freshwater planarian *Schmidtea mediterranea* identify major cell types and pathway conservation. *Genome Biol*. 19(1):124.

Thiel D, Franz-Wachtel M, Aguilera F, Hejnol A. 2018. *Xenacoelomorph neuropeptidomes* reveal a major expansion of neuropeptide systems during early bilaterian evolution. *Mol Biol Evol*. 35(10):2528–2543.

Tyler S. 1976. Comparative ultrastructure of adhesive systems in the turbellaria. *Zoomorphologie* 84(1):1–76.